EPJ Web of Conferences **223**, 01005 (2019) https://doi.org/10.1051/epjconf/201922301005
*NSD2019*

# Structure and reactions of N=7 isotones: parity inversion and transfer processes

*Francisco* Barranco[1,*], *Ricardo A.* Broglia[2,3,**], *Gregory* Potel[4,***], and *Enrico* Vigezzi[5,****]

[1]Departamento de Física Aplicada III, Escuela Superior de Ingenieros, Universidad de Sevilla, Sevilla, Spain
[2]The Niels Bohr Institute, University of Copenhagen, Copenhagen, Denmark
[3]Universitá degli Studi di Milano, Milano, Italy
[4]National Superconducting Cyclotron Laboratory, Michigan State University, East Lansing, USA
[5]Istituto di Fisica Nucleare, Sezione di Milano, Milano, Italy

**Abstract.** The interplay of particle and vibrations in N=7 isotones is considered according to nuclear field theory, focusing on the main many-body effects which renormalise the energy spectrum of the halo nucleus $^{11}$Be, leading to parity inversion and to renormalization of the form factors determining the cross sections associated with one-nucleon transfer reactions.

## 1 Introduction

Many features of the N=7 halo nuclei $^{10}$Li and $^{11}$Be can be understood taking into account the strong many-body renormalization effects arising from the coupling of particles with the quadrupole collective vibrations of the core. In particular, this coupling leads to the inversion of the sequence of the $\frac{1}{2}^+$ and $\frac{1}{2}^-$ levels, as compared to the usual shell model order. In this contribution we outline the treatment of these many-body effects and the results obtained, also for other N=7 isotones, within nuclear field theory (NFT) [1–4], which has been shown to lead to a rather accurate description of the structure and reactions measured in these nuclei, in particular reproducing the absolute cross sections of the $^{10}$Be(d,p)$^{11}$Be and $^{9}$Li(d,p)$^{10}$Li transfer reactions [5, 6].

## 2 The model Hamiltonian

The starting Hamiltonian is $\mathcal{H} = H'_{sp} + H_{tb}$, where $H'_{sp}$ is a one-body term and $H_{tb}$ is the two-body (four-point vertex) interaction. The free (bare) fermion fields are the Hartree-Fock solution ($H_{sp}$) of $\mathcal{H}$. In the resulting (particle-hole) basis the collective (quadrupole) states are to be calculated by diagonalising $H_{tb}$ in the random phase approximation (RPA). The corresponding solutions provide, aside from the collective Hamiltonian $H_{coll}$, the particle-vibration coupling vertices ($H_{PVC}$). These vertices and the two-body interaction should be allowed to act in all orders of perturbation theory to generate the variety of Feynman diagrams leading to the renormalisation of the single-particle and collective (free fields) modes and their interweaving, with the proviso of eliminating the contribution of virtual unperturbed loops (bubbles). Expressing it differently, one is confronted with the task of diagonalising the second term of the Hamiltonian $H = (H_{sp} + H_{coll}) + (H_{PVC} + H_{tb})$ in a basis consisting of single-particles and collective states, with the proviso of eliminating from the initial and final states particle (and hole) configurations which can be replaced by collective modes.

In what follows, we implement this program in connection with a series of $N = 7$ isotones, in terms of the program of renormalized NFT [3]. The one which parallels that of QED in the case of single-particle states: the bare energies are adjusted so that the dressed (renormalized) single-particle states best reproduce the experimental findings [5]. Empirical renormalization (see e.g. [3]) concerning collective motion is adopted. In particular we will calculate the quadrupole vibrations by diagonalizing in the RPA and in an empirical single-particle basis (Woods-Saxon parametrization as found in Eq. (2-181) of ref. [7]) a separable interaction tuned to reproduce the properties of the low lying modes. Within this approximation, the particle-vibration coupling form factor in the case of quadrupole vibrations is $\delta V_2(r)Y_{2\mu}(\hat{r})$, where $\delta V_2(r) = -\beta_2 R_0 dV/dr$. It is of notice that we will not consider those diagrams which renormalise the phonon states, in keeping with the fact that such diagrams lead to results which reproduce the experimental findings [8]. Furthermore, we will neglect the four point (fermion) vertices, as it is known that their contribution is small.

Although it is possible to iterate the desired processes to infinite order of perturbation theory, a useful parameter to assess the order of a graphic contribution is $1/\Omega$, $\Omega$ being the effective degeneracy of the model space (number of Kramers degenerate levels available to the particles lying

*e-mail: barranco@us.es
**e-mail: broglia@mi.infn.it
***e-mail: potel@nscl.msu.edu
****e-mail: vigezzi@mi.infn.it

close to the Fermi energy). The order of a given diagram is given by $n_\Omega = n_\Lambda/2 - n_f + n_{tb}$, where $n_f$, $n_\Lambda$, $n_{tb}$ are the number of fermion loops over which summation can be carried out, the number of particle-vibration coupling vertices and the number of four-point vertices respectively.

The configurations including one or more phonons lie outside the single-particle (basic) space, and enter the calculations as intermediate, virtual states, their energies appearing in the energy denominators of the Feynman diagrams. This procedure leads to an energy-dependent self-energy function, producing a much greater number of solutions than the dimension of the explicit single-particle basis. The square amplitude of the single-particle component associated with each solution is in general smaller than one, reflecting the fact that the renormalised states contain admixtures with collective phonons. The 'hidden' configurations containing one or more phonons may be explicitly reconstructed following the Bloch-Horowitz formalism (see App. B of [1]).

The parameters of the mean field $H_{sp}$ are chosen so as to give an optimal global fit to the experimental energy spectra in the $N = 7$ isotones $^{10}$Li,$^{11}$Be, $^{12}$B and $^{13}$C, after many-body renormalisation effects are taken into account. This bare mean field is parametrised as a Saxon-Woods potential well, characterised by the well depth $V_{WS}$, the diffuseness $a_{WS}$, the radius $R_{WS}$ and by the spin-orbit strength parameter $V_{LS}$, as well as by a $r-$dependent effective mass. We obtain the values $V_{WS} = -82 + 54(N-Z)/A$ MeV, $a = 0.75$ fm, $R_{WS} = 0.99\, A^{1/3}$ fm and $V_{LS} = 0.3\, V_{WS}$. We will be particularly interested in the renormalization of $s_{1/2}$, $p_{1/2}$ and $d_{5/2}$ orbitals lying above the Fermi energy $E_F$. The renormalized radial wavefunction associated with these states will be denoted by $\tilde{R}_{ai}(r)$, where $a \equiv \{lj\}$, while $i$ labels the various solutions. It obeys the equation

$$H_{sp}\tilde{R}_{ai}(r) + \int dr' \Sigma_a(r, r', \tilde{E}_{ai})\tilde{R}_{ai}(r') = \tilde{E}_{ai}\tilde{R}_{ai}(r), \quad (1)$$

where $\Sigma_a(r, r', \tilde{E})$ denotes the self-energy. This is a complex, non local, energy-dependent quantity, which represents the interaction between the odd neutron (halo neutron in the case of $^{10}$Li and $^{11}$Be) and the core, and is an essential element to compute the single-particle transfer cross sections together with the optical potentials in the entrance and exit channels. Within this context $\Sigma$ is the structure input needed to calculate the polarisation contribution to the optical potential.

## 3 Many-body renormalization effects

The self-energy in the first order of perturbation in $1/\Omega$, i.e. including only intermediate configurations containing one phonon, can be written explicitly as a sum over the unperturbed wave functions and energies $R^{WS}_{ai}$ and $E_{ai}$ calculated in the (bare) Saxon-Woods potential well,

$$\Sigma_a(r, r', \tilde{E}) = \sum_{bi} \frac{\Xi^2_{a,b\lambda} R^{WS}_{bi}(r') R^{WS}_{bi}(r) \delta V(r') \delta V(r)}{\tilde{E} - (E_{bi} + \hbar\omega - i\eta)} + \sum_{ci} \frac{\Xi^2_{a,c\lambda} R^{WS}_{ci}(r') R^{WS}_{ci}(r) \delta V(r') \delta V(r)}{\tilde{E} + (E_{ci} + \hbar\omega - i\eta)}, \quad (2)$$

where ($E_{bi} > E_F; E_{ci} < E_F$), while $\Xi_{a,b\lambda}$ denote angular momentum recoupling factors. We have included continuum states up to 50 MeV, calculated in a box of radius equal to 50 fm, checking that this leads to converged results, within 100 keV, for the energy of the renormalised states. Note that expressions analogous to that of Eq. (2), i.e. of second order in $\beta_2$, appear in a number of many-body approaches in the calculation of the self-energy. The first term accounts for correlations due to $H_{PVC}$ and acts mostly on the bound $2s_{1/2}$ state and on the $d_{5/2}$ levels lying in the continuum, while the second one accounts for the blocking of core ground state correlations and strongly renormalizes the $1p_{1/2}$ state, due to the quadrupole coupling to the $1p_{3/2}$ hole state. The first-order results are schematically shown in Fig. 1 (2nd column), where it can be seen that the inversion between $1/2^+$ and $1/2^-$ levels is reproduced. The different renormalized states ($i = 1, 2, ...$) of angular momentum and parity $j^\pi$ will be denoted by $\widetilde{j^\pi_i}$, their energy by $\widetilde{E}_{j^\pi_i}$, and their amplitude over a single-particle state $k$ by $(\widetilde{a}_{j^\pi})_{ik}$. The sum of the amplitudes squared $\widetilde{A^2}_{j^\pi_i} \equiv \sum_k (\widetilde{a}_{j^\pi})^2_{ik}$ for the states $\widetilde{j^\pi_i} = \widetilde{1/2}^+_1, \widetilde{1/2}^-_1$ is equal to 0.93 and 0.85 respectively, reflecting the sizeable admixture of the $2^+$ phonon in the wavefunctions. The $5/2^+$ phase shifts show a resonance lying at an energy several MeV lower than its unperturbed value calculated with the bare potential.

In many applications, the processes described by Eq. (2) are sufficient to obtain a reasonable description of experimental data, in particular in heavy spherical nuclei ($\Omega \approx 6-8$ for $A \approx 120$ and $\Omega \approx 8-10$ for $A \approx 200$). In the case of the N=7 isotones under study, for which $\Omega \approx 3-5$, it turns out that further orders in the perturbation series have to be included in order not to miss important renormalization effects on specific configurations, as it will be shown below.

Substituting the unperturbed WS energies and wavefunctions $E_{bi}, R^{WS}_{bi}$ appearing in Eq. (2) with perturbed ones to be determined, leads to a more complex expression for the self-energy, involving the unknown energies for states of different angular momentum, and the resulting equations should be solved simultaneously and consistently for all of them. This amounts to the summation of the so called rainbow series to infinite order (see Fig. 2), including configurations with an arbitrarily large number of phonons, subject only to the restriction of no crossing among them. An important property of this series is the systematic coherence of all the terms. Contributions involving configurations containing crossing phonons (vertex corrections) imply recoupling factors of varying sign, which in general cause strong cancellations, leading to smaller contributions, which we neglect.

The rainbow series can be summed to infinite order making use of the *empirical renormalization* method for the intermediate states in Eq. (2). This should represent a reasonable approximation, if the renormalized energies and wavefunctions resulting from Eq. (1) turn out to be indeed close to the experimental data, as has been extensively tested in ref. [8]. In practice, we implement it by calculating Eq. (2) inserting energies and wave functions

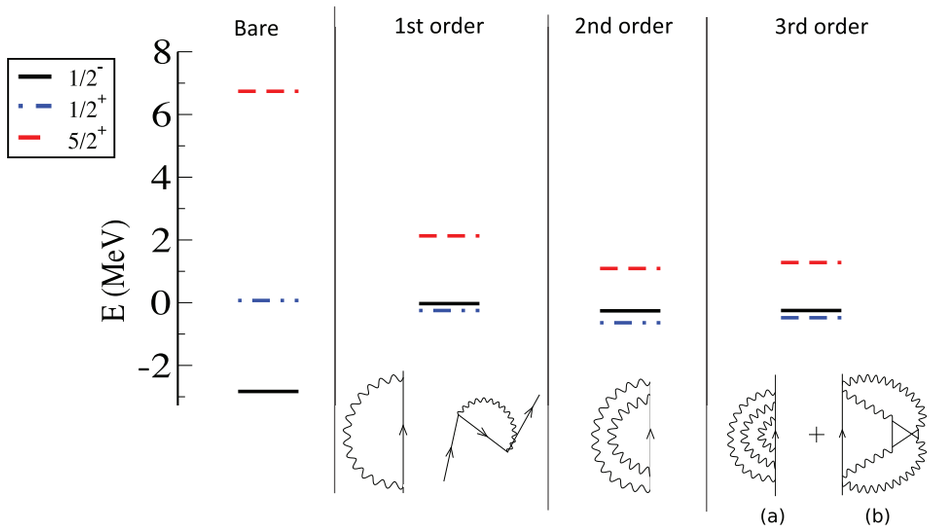


**Figure 1.** (color online) Theoretical spectrum of low-lying states of $^{11}$Be, calculated in different perturbation orders in NFT. The lowest $1/2^-$,$1/2^+$ and $5/2^+$ levels are shown by solid, dot-dashed and dashed lines respectively. In the case of $5/2^+$, the energy of the resonant state is indicated. Representative diagrams included at each order are drawn at the bottom of the figure.

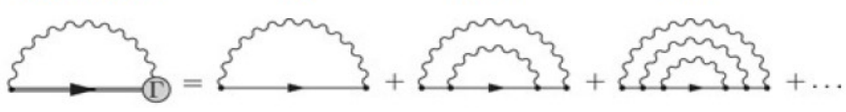

**Figure 2.** The rainbow series.

obtained from the empirical Saxon-Woods potentials mentioned above [7].

We then obtain that the summation of the rainbow series leads to a rather dramatic effect for the $\widetilde{5/2}^+_1$ state, which has a resonant, many-body character, displaying an admixture with the $s_{1/2} \otimes 2^+$ and $d_{5/2} \otimes 2^+$ configurations as large as 50%. This state becomes almost bound ($\widetilde{E}_{5/2^+_1}$ = 0.6 MeV), in contradiction with experimental data (1.3 MeV). This strong effect is mostly due to the fact that the virtual $2s_{1/2}$ state entering the rainbow series is bound (empirical renormalization, $E_{1/2^+}$= -0.5 MeV), leading to a enhanced coupling of the $\widetilde{5/2}^+_1$ state with the $s_{1/2} \otimes 2^+$ configuration, as compared to the first order, in which the $s_{1/2}$ state is calculated in the bare potential and lies in the continuum. The coupling of the $\widetilde{1/2}^+_1$ state with the $d_{5/2} \otimes 2^+$ configuration is also enhanced, and the value of $\widetilde{A^2}_{1/2^+_1}$ goes from 0.93 to 0.76.

Physically, the reason for these strong effects is the overcounting of the correlations appearing when two or more quadrupole phonons are present, as in rainbow-like processes. In other words, RPA phonons are quasi-bosons with an underlying fermionic structure, which eventually lead to Pauli principle corrections when two or more of them are present in a given configuration. The relevance of this interference increases as the p-h Hilbert configuration space becomes smaller, which is the case for light nuclei, where the density of bound/resonant levels is rather low. In the present case such problems manifest themselves first in the third order of perturbation, in keeping with the sensible results obtained for the $\widetilde{5/2}^+_1$ state in second order, obtained iterating the first order results ( $\widetilde{E}_{5/2^+_1}$= 1.1 MeV, see Fig. 1, third column). In fact, Pauli blocking effect appears in the self-energy at the third order in $1/\Omega$, through the so called butterfly diagrams, shown in the bottom part of Fig. 1 (4th column, (b)). In $^{11}$Be, these

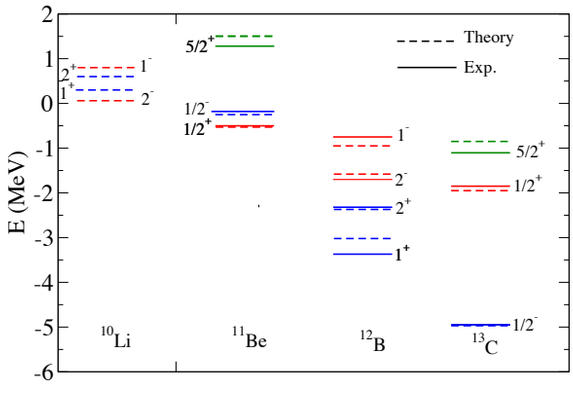


**Figure 3.** (color online) The experimental energies of the low-lying states in the $N$ = 7 isotones $^{11}$Be, $^{12}$B and $^{13}$C are displayed by solid lines. The corresponding theoretical energies are shown by dashed lines. Also shown are the predictions in $^{10}$Li. States based on $1/2^-$, $1/2^+$ and $5/2^+$ neutron configurations are shown by blue, red and green lines respectively.

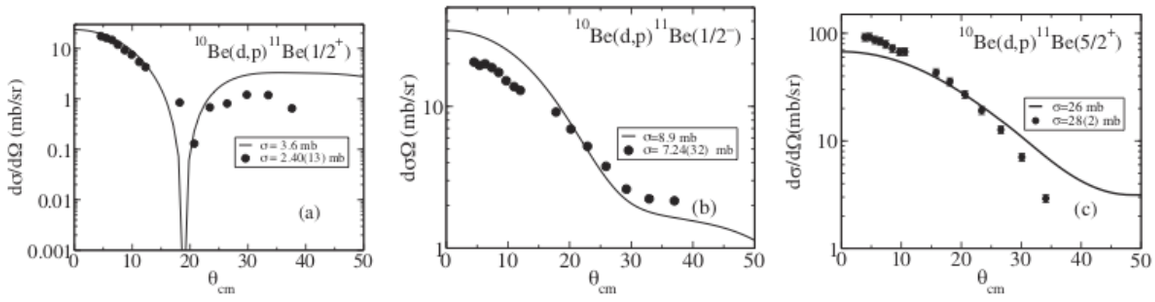


**Figure 4.** From [5]. Absolute differential and (insets) integrated cross sections associated with the reactions d($^{10}$Be,$^{11}$Be)p at E = 107 MeV, populating the $1/2^+$, $1/2^-$ and $5/2^+$ low-lying states. The experimental data [9] are displayed in terms of solid dots.

diagrams increase the energy of the $2^+_1 \otimes 2^+_1$ two-phonon configuration by about 2.5 MeV, and decrease the value of the quadrupole deformation parameter $\beta_2$ by about 25%. Depending on the extent that the two phonon configuration appears in the rainbow series, the effect of the anharmonicity differs considerably from one partial wave to the other. Its contribution is particularly relevant for the $\widetilde{5/2}^+_1$ state, increasing its energy by 0.7 MeV and bringing the empirical renormalization result to $\widetilde{E}_{5/2^+_1}$= 1.3 MeV, in agreement with the experimental data. This result coincides with energy calculated in perturbation, which increases by 0.2 MeV going from the second order to the third order, as a result of an attractive contribution of -0.5 MeV arising from diagram (a), and a repulsive one of +0.7 MeV due to diagram (b) (see Fig. 1, fourth column). Third order effects on the $\widetilde{1/2}^+_1$ state are modest and those on the $\widetilde{1/2}^-_1$ state are even weaker. Finally, one obtains $\widetilde{A^2}_{1/2^+_1}$ = 0.86 and $\widetilde{A^2}_{1/2^-_1}$ = 0.83. Overall, the results displayed in Fig. 1 testify to the convergence of the NFT results already at third order of perturbation theory.

It is of notice that the sensitivity of the $\widetilde{5/2}^+_1$ state to corrections beyond the first order is in keeping with the fact that, in order to reproduce the energy of this state in other theoretical schemes, important changes in the spherical mean field or the introduction of a deformed mean field are required. We furthermore remark that the effects discussed above are associated with many-body phenomena (core excitation), and their occurrence in microscopic models should be rather independent of the N-N interaction used.

The renormalized energies of $^{11}$Be as well as of $^{13}$C are compared to experimental data in Fig. 3. The calculated wave functions and associated self-energies have been used to calculate one-particle cross sections [5], resulting in an overall agreement with the data. In Fig. 4 the calculated cross sections associated with the reactions d($^{10}$Be,$^{11}$Be)p at E=107 MeV performed in inverse kinematics, populating the $1/2^+$, $1/2^-$ and $5/2^+$ states are shown and compared with experimental data [9].

## 4 The case of odd-odd nuclei

In the case of the N=7 isotopes $^{12}_{5}$B and $^{10}_{3}$Li, which have an odd number of protons, one needs to take into account the interaction of this proton with the renormalized neutron, before being able to compare the NFT results with experiment. In fact the coupling of the $1p_{3/2}$ proton with the neutron $\widetilde{1/2}^+_1$ and $\widetilde{1/2}^-_1$ states leads in either case to a doublet, namely $1^-$ and $2^-$, and $1^+$ and $2^+$ respectively, while its coupling with the $\widetilde{5/2}^+_1$ neutron state leads to a $1^-, 2^-, 3^-$ and $4^-$ quadruplet. These multiplets are degenerate in the mean field approximation, while they are splitted according to experiment. An accurate theoretical description of such splittings requires an accurate consideration of the n-p interaction. We have limited ourselves to the use of a rather simple, but extensively employed version of a zero range force [10], containing a direct and a spin dependent term. The resulting levels and splittings are shown in Fig. 3. In all these result the empirical renormalization and the anharmonicity corrections described above have been included. The comparison with data is rather satisfactory. The calculation of transfer cross sections using the calculated renormalized wavefunctions (form factors) and associated self-energies are in progress [6].

## 5 Acknowledgment

F.B and E.V. acknowledge funding from the European Union Horizon 2020 research and innovation program under Grant Agreement No. 654002. F.B. acknowledges funding from the Spanish Ministerio de Economía under Grant Agreement No. FIS2017-88410-P.

## References

[1] D.R. Bès et al., Nucl. Phys. **A260** 1 (1976)
[2] P.F. Bortignon et al., Phys. Rep. **30C** 305 (1977)
[3] R.A. Broglia et al., Phys. Scr. **91** 063012 (2016)
[4] D.R. Bès, Phys. Scr. **91** 03010 (2016)
[5] F. Barranco et al., Phys. Rev. Lett. **119**, 082501 (2017)
[6] F. Barranco et al., arXiv:1812.01761
[7] A. Bohr and B.R. Mottelson, *Nuclear Structure*, Vol. I, Benjamin, New York (1969)
[8] A. Idini et al., Phys. Rev. C **92**, 031304(R) (2015)
[9] K.T. Schmitt et al, Phys. Rev. C **88**, 064612 (2013).
[10] K. Heyde, *The nuclear shell model*, Springer-Verlag (1990)